Elimination of the Inner-Shell Lifetime Broadening in X-Ray-Absorption Spectroscopy

K. Hämäläinen,[a] D. P. Siddons, J. B. Hastings, and L. E. Berman
National Synchrotron Light Source, Brookhaven National Laboratory, Upton, New York 11973
(Received 9 August 1991)

A novel method to measure x-ray-absorption spectra without the inner-shell lifetime broadening is presented. It is based on a high-resolution spectrometer which can be used to analyze the fluorescence photon energy with better resolution than the natural linewidth. The dramatic improvement in resolution and detailed structure for the x-ray-absorption near-edge structure (XANES) at the Dy L_{III} edge is presented. This new technique reveals structure which is totally invisible using conventional XANES.

PACS numbers: 78.70.En, 32.30.Rj, 61.10.Lx

In x-ray-absorption spectroscopy the variations in absorption are measured by scanning the energy of the incident photon beam while monitoring the transmitted beam, the fluorescence radiation, or the nonradiative decay. If the kinetic energy of the ejected photoelectron is less than about 100 eV, the measured spectrum can give information about the density of unoccupied states above the Fermi level, which is sensitive to the bonding, oxidation, and coordination of the system. With higher photoelectron energies the backscattering from neighboring atoms creates oscillatory structure and gives local structural information even in disordered systems [extended x-ray-absorption fine structure (EXAFS) [1]].

As the number of synchrotron facilities and beam lines has rapidly increased, EXAFS has remained one of the most utilized tools at these facilities. However, the increased flux from the dedicated storage rings has not provided improved energy resolution because the limit has been the natural lifetime broadening of the core hole, not the incident beam resolution. In the K-shell photoabsorption process, for example, the incident photon ejects the K-shell electron to the unoccupied states, and since this hole has a finite lifetime the hole is filled by an outer-shell electron leading, in the case of the radiative decay, to fluorescence radiation. The Heisenberg uncertainty principle gives rise to an energy uncertainty inversely proportional to the lifetime. For the K shell [2] the energy width increases almost exponentially as a function of Z varying from 1 eV (V, $Z=23$) up to 40 eV (W, $Z=74$) and for the L_{III} shell from 3.7 eV (Nd, $Z=60$) up to 7.4 eV (U, $Z=92$). For these edges, therefore, an incident beam resolution better than the nominal 1-eV limit has not been crucial.

Attempts to overcome this limitation have been made previously using coincidence techniques [3] in photoemission spectroscopy which probes the occupied levels, in x-ray emission spectroscopy [4], and in x-ray-absorption near-edge spectroscopy (XANES) by measuring the resonant Raman scattering (RRS) differential cross section [5]. In the present work we have performed a normal fluorescence XANES measurement by scanning the incident energy across an absorption edge but monitored the fluorescence intensity using an analyzer with better resolution than the natural lifetime width. We observe dramatically enhanced resolution in the case of the dysprosium L_{III} edge when compared with a conventional transmission XANES measurement from the same sample.

The experiment was carried out on the X25 hybrid wiggler beam line at the National Synchrotron Light Source, at the Brookhaven National Laboratory. The beam-line optics consist of a Pt-coated double-focusing mirror collecting about 1.5 mrad of the horizontal opening angle and a two-crystal Si(220) monochromator. The incident beam at the sample had a spot size of less than 1 mm^2, a measured energy resolution of 0.7 eV at 6.5 keV, and a monochromatic flux of about 10^{11} photons/s.

The spectrometer used to measure the fluorescence is based on a spherically bent perfect Si(440) crystal and a position-sensitive detector (PSD) sitting on the same Rowland circle as the sample. The fluorescence radiation was measured at 90° scattering angle in the vertical plane. This experimental setup made it possible to decrease the size of the incident beam (source size for the analyzer) and to improve the incident beam resolution simultaneously by simply reducing the upstream beam vertical apertures. The diameter of the Rowland circle was 900 mm and the full length of the PSD (100 mm) enabled measurements over the angle range of $\theta=83.3°-86.5°$ corresponding to energies from 6501 to 6469 eV without moving the detector. The spatial resolution of the gas-proportional-counter-based PSD was 200 μm corresponding to 60 meV, and its energy resolution was adequate to discriminate the harmonic contamination in the incident beam [6]. The use of the PSD was not crucial to the experiment, but it proved to be very useful for calibration and adjustment of the instrument. The measured resolution of the analyzer was 0.3 eV at 6.5 keV.

Using this arrangement, the L_{III} edge of dysprosium ($Z=66$) was studied. Three different samples were used: dysprosium metal (100-μm foil), nitrate, and oxide (thin powder samples between two Kapton windows). The energy of the fluorescence radiation was analyzed by rotating the analyzer crystal which focuses a 0.3-eV bandwidth of the radiation to the PSD. Figure 1 shows the measured Dy $L\alpha_1$ fluorescence line ($E_{M_V}-E_{L_{III}}=6495$ eV) from $Dy(NO_3)_3$ when the incident energy was 50 eV above the L_{III} absorption edge ($E_{L_{III}}=7790$ eV). The cutoff on the high-energy side is due to the spectrometer

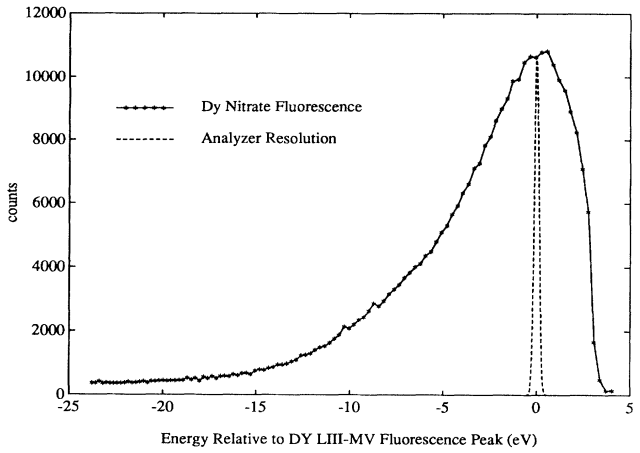

FIG. 1. Measured dysprosium $L\alpha_1$ ($L_{III}M_V$) fluorescence line shape (solid line). The dashed line corresponds to the instrumental resolution (0.3 eV) of the analyzer. Time per data point is 1 min.

vacuum chamber wall which limited the highest detectable photon energy (lowest Bragg angle). Theoretical values for the atomic energy shell widths are 4.2 eV ($\Gamma_{L_{III}}$) and 1.4 eV (Γ_{M_V}) [2]. These values, taken together with the analyzer resolution, would predict a slightly narrower linewidth than the one measured. However, the energy levels in solids are expected to be broader than in the atomic case due to numerous nonlifetime effects [2].

In order to demonstrate the enhanced resolution, identical incident energy scans from the same $Dy(NO_3)_3$ sample using conventional EXAFS techniques and high-resolution fluorescence analysis were performed. In the former case the total absorption was monitored with an ionization chamber after the sample, and in the latter case only the narrow bandwidth of the total fluorescence radiation indicated by the dashed line in Fig. 1 was monitored. Figure 2 shows the measured partial fluorescence intensity (solid line) and the absorption coefficient based on the transmission measurement (dashed line) normalized to the same values well below and above the absorption edge. The high-resolution XANES reveals a well separated true absorption edge followed by the white line corresponding to strong dipole-allowed transitions to empty $5d$ states. In the conventional XANES the edge is smeared out. Even though the white line structure is reduced in width, it is not correspondingly higher than in the transmission case. This is because the fluorescence measurement is not corrected for sample absorption (saturation effect). The first edge, clearly separated from the white line, corresponds to the real absorption edge originating from the quadrupole-allowed transition from $2p$ to the partially filled $4f$ states. This feature is almost completely obscured by the lifetime broadening in the transmission spectrum.

This enhanced resolution is easily understood. When

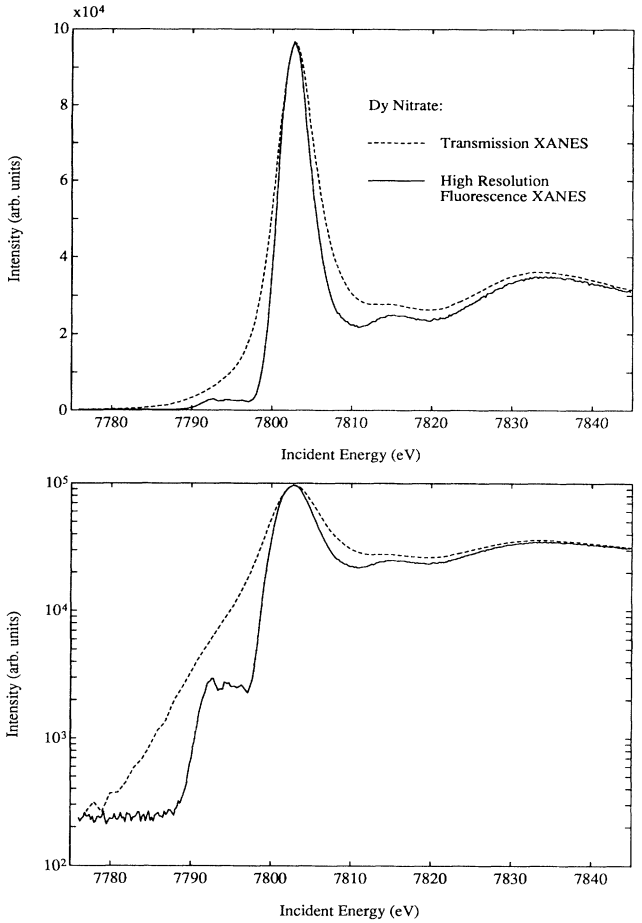

FIG. 2. XANES spectrum of Dy L_{III} edge in dysprosium nitrate measured using the high-resolution technique and the conventional transmission XANES technique. Both measurements were accomplished using the same sample and with the same incident photon energy resolution.

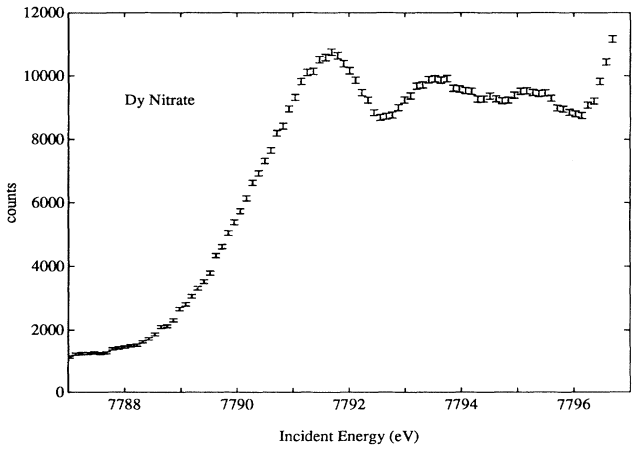

FIG. 3. Measured XANES spectrum of $Dy(NO_3)_3$ just above the Dy L_{III} edge which corresponds to quadrupole transitions of $2p$ electrons to the unoccupied $4f$ states.

the energy of the incident photon is tuned across an absorption edge, a resonant increase in the intensity of the scattered radiation is observed [7]. This behavior can be explained by a second-order scattering process arising from the $\mathbf{p}\cdot\mathbf{A}$ term of the interaction Hamiltonian. Both this resonant Raman scattering and fluorescence radiation can be described by a single formula [8]. The intermediate state in this process involves an inner-shell hole with a finite lifetime giving rise to a Lorentzian broadening of the emission line. This uncertainty in the inner-shell energy makes it possible to detect "fluorescence radiation" with incident photon energies below the absorption edge. According to a semiclassical interpretation [9] this RRS can simply be described as a fluorescence process following creation of a hole in the tail of the lifetime-broadened energy shell.

The differential cross section for the LM fluorescence due to dipole transition, for example, can be written as

$$\frac{d\sigma}{d\omega_2}=\frac{2\pi\hbar r_0^2}{m^2}\left(\frac{\omega_2}{\omega_1}\right)\int d\epsilon\left(\frac{dN}{d\epsilon}\right)\int d\Omega|\langle(2p)(3d)^{-1}|\mathbf{e}_2\cdot\mathbf{p}|(2p)^{-1}(3d)\rangle|^2$$
$$\times\int d\Omega_\epsilon|\langle(\epsilon\mathbf{p})|\mathbf{e}_1\cdot\mathbf{p}|(2p)\rangle|^2$$
$$\times\frac{1}{(E_M-E_L-\hbar\omega_2)^2+\Gamma_L^2/4}\,\frac{\Gamma_M}{(\hbar\omega_1-\hbar\omega_2+E_M-\epsilon)^2+\Gamma_M^2/4}\,, \tag{1}$$

where $\hbar\omega_1$ and $\hbar\omega_2$ are the incident and scattered photon energies (polarization vectors $\mathbf{e}_1$ and $\mathbf{e}_2$, respectively), E_L and E_M the L- and M-shell binding energies, $\mathbf{p}$ the electron momentum operator, $dN/d\epsilon$ the final density of states of the photoelectron ejected to the solid angle of $d\Omega_\epsilon$ with kinetic energy of ϵ, and Γ_L and Γ_M the total lifetime widths for the L- and M-shell holes.

According to Eq. (1) the RRS spectrum has a Lorentzian shape with a high-energy cutoff at $\hbar\omega_2=\hbar\omega_1+E_M$ resulting from the energy conservation requirement and is smeared by the final M-shell lifetime width Γ_M. When the incident photon energy is well above the absorption edge, the resulting fluorescence has a Lorentzian line shape with FWHM of $\Gamma_L+\Gamma_M$. However, close to the edge the cutoff leads to an emission line that has a narrower linewidth than the lifetime limited fluorescence radiation [10] and far below the edge the emission line is a broad truncated Lorentzian. Furthermore, oscillations of the photoelectron transition matrix element and the unoccupied density of states have recently been observed in a high-resolution RRS spectrum [5].

When the incident energy is tuned across the L-absorption edge and the fluorescence signal is monitored with an energy bandwidth of $B(\omega_2)$, the measured intensity is proportional to the cross section

$$\sigma(\omega_1)=\left(\frac{\Gamma_{L,R}}{\Gamma_L}\right)\int_0^\infty d(\hbar\omega_2)\int_0^\infty d\epsilon B(\omega_2)\left(\frac{\omega_2}{\omega_1}\right)\frac{E_M-E_L+\hbar\omega_1-\hbar\omega_2}{E_M-E_L}\,\frac{\Gamma_L/2\pi}{(\hbar\omega_1+E_L-\epsilon)^2+\Gamma_L^2/4}$$
$$\times\frac{\Gamma_M/2\pi}{(\hbar\omega_1+E_M-\hbar\omega_2-\epsilon)^2+\Gamma_M^2/4}\,\sigma_L(-E_L+\epsilon)\,, \tag{2}$$

where we have adopted the standard definitions for the L-shell radiative width $\Gamma_{L,R}$ and for the total L-shell photoabsorption cross section σ_L [proportional to the first and the second matrix elements in Eq. (1), respectively].

When the fluorescence radiation is measured with a solid-state detector, the accepted bandwidth $B(\omega_2)$ due to the instrumental resolution is clearly much wider than the natural energy width of the L-shell hole. However, if the fluorescence photon energy can be measured with resolution better than Γ_L, the Lorentzian lifetime broadening is suppressed by $B(\omega_2)$ and sharper features in XANES spectra can be seen when the incident energy is scanned in the vicinity of an absorption edge. The spectral structure of σ_L is still smeared by the M-shell lifetime width which, in general, is much sharper (longer lifetime) than the L-shell hole.

Not only does this technique sharpen the conventional XANES, but Fig. 2 shows structure between the absorption edge and the white line which is not visible in the transmission spectrum. Therefore a more careful study in this energy region was carried out and is shown in Fig. 3. This figure reveals clear structure which is not observable using conventional x-ray-absorption spectroscopy. Note that the incident flux and the efficiency of the spectrometer are high enough to probe even the weak quadrupole transition and data of good statistical accuracy can be achieved in reasonable times (in Fig. 3 each point corresponds to 6.5-min total measurement time).

To further demonstrate the broad applicability of this method some high-resolution studies of different dysprosium compounds were performed. Figure 4 shows the measured XANES spectra from Dy metal, oxide, and nitrate. In all cases the position of the real absorption edge corresponding to the $4f$ density of states seems to be independent of the chemical environment, while the white line structure due to the unoccupied $5d$ levels is much more sensitive to the chemical changes. Both the position and

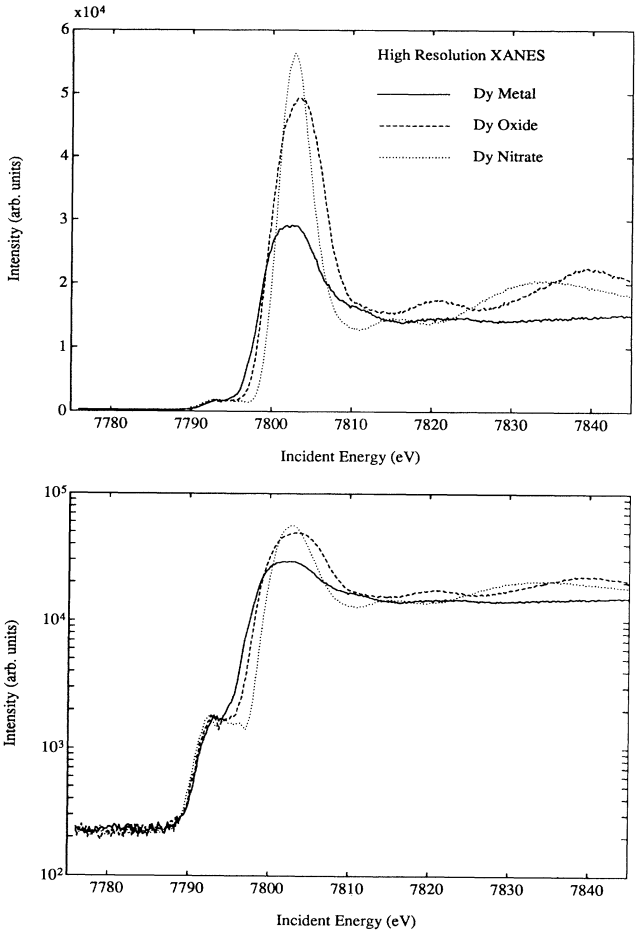

FIG. 4. Comparison of high-resolution spectra for dysprosium metal (solid), Dy_2O_3 (dashed), and $Dy(NO_3)_3$ (dotted).

the half-width of the white line are clearly changed in these cases. More careful studies on the fine structure of the $4f$ density of states were also carried out which showed that at least the first, and partly the second, peak observed in the nitrate spectrum (see Fig. 3) exists in the case of the metal and of the oxide. Unfortunately, in the case of the oxide, and especially in the metal, the white line starts to overlap the $4f$ density-of-states structure.

These measurements demonstrate that with high-resolution energy analysis of the fluorescence radiation the lifetime broadening in x-ray-absorption spectroscopy can be overcome. The present resolution opens new possibilities for XANES studies and can be applied to EXAFS measurements as well. EXAFS studies can give information on the local atomic environment, but its range is limited to a few interatomic distances due to the natural backscattering amplitude damping and Debye-Waller damping. However, in some cases the exponential damping originating from the Lorentzian line shape of the core hole is the major limitation for the EXAFS range and in these cases the high-resolution fluorescence spectroscopy could be particularly useful. Furthermore, if the emission line has some satellite structure related to the numerous solid-state effects concerning the final-state hole, the high-resolution probe can be used to perform interesting absorption studies which are sensitive to this final-state structure.

There is no doubt about the superiority of the new high-resolution technique, but there are still some limitations to overcome before it becomes a routinely utilized spectroscopic tool. It is important to appreciate that high resolution demands extremely high incident flux to get reasonable count rates. Our signal rate, 500 counts/s from the Dy sample at the fluorescence peak, was achieved with a state-of-the-art focusing wiggler beam line. The next generation synchrotron sources with even higher fluxes and brightnesses should make this technique routine.

The authors would like to acknowledge S. Cramer, C. Kao, and V. Stojanoff for ideas, discussion, and help during the experiment. This work was supported by the U.S. Department of Energy under Contract No. DE-AC02-76CH00016 and one of the authors (K.H.) is indebted to the Finnish Academy for financial support.

[a]Permanent address: Department of Physics, University of Helsinki, Siltavuorenpenger 20D, SF-00170 Helsinki, Finland.

[1] *EXAFS Spectroscopy,* edited by B. K. Teo and D. C. Joy (Plenum, New York, 1981).

[2] M. O. Krause and J. H. Oliver, J. Phys. Chem. Ref. Data **8**, 329 (1979).

[3] E. Jensen, R. A. Bartynski, S. L. Hulbert, E. D. Johnson, and R. Garret, Phys. Rev. Lett. **62**, 71 (1989).

[4] P. L. Cowan, Phys. Scr. **T31**, 112 (1990), and references therein.

[5] P. Suortti, V. Eteläniemi, K. Hämäläinen, and S. Manninen, J. Phys. (Paris), Colloq. **48**, C9-831 (1987).

[6] G. C. Smith, Nucl. Instrum. Methods Phys. Res., Sect. A **222**, 230 (1984).

[7] C. J. Sparks, Phys. Rev. Lett. **33**, 262 (1974).

[8] T. Åberg and J. Tulkki, in *Atomic Inner-Shell Physics,* edited by B. Crasemann (Plenum, New York, 1985), Chap. 10.

[9] K. Hämäläinen, S. Manninen, P. Suortti, S. P. Collins, M. J. Cooper, and D. Laundy, J. Phys. Condens. Matter **1**, 5955 (1989).

[10] P. Eisenberger and P. M. Platzman, Phys. Rev. Lett. **36**, 623 (1976).